Available online at www.sciencedirect.com
ScienceDirect
Journal of Power Sources 162 (2006) 977–984
JOURNAL OF POWER SOURCES
www.elsevier.com/locate/jpowsour

Photographic production of metal nano-particles for fuel cell electrodes

Juan Jiang *, Timothy D. Hall, Loukas Tsagalas, Davide A. Hill, Albert E. Miller

Department of Chemical and Biomolecular Engineering, University of Notre Dame, 182 Fitzpatrick Hall, Notre Dame, IN 46556, USA

Received 11 July 2006; accepted 19 July 2006
Available online 28 August 2006

Abstract

A photographic Pt printing process has been used to prepare catalysts for fuel cell applications. Ferric oxalate was used as a UV sensitizer, absorbing UV energy and converting Fe^{3+} to Fe^{2+}, which then reduces metal catalyst ions, such as Pt or Pd ions to metals in the presence of a developer, such as ammonium citrate. Transmission electron microscope (TEM) and scanning electron microscope (SEM) studies revealed that Pt particles smaller than 5 nm were formed, however, the particles tended to aggregate and form clusters up to 300 nm. A deposition efficiency of 16% was obtained when Pt was printed on Nafion membranes. The catalytic performance of the photo-printed Pt was evaluated using a single H_2 fuel cell. The mass-specific electrochemical area of the catalyst, H_2 crossover rate through the Pt-printed membrane and the membrane resistance were measured. At 60 °C, a peak power density of 75 mW cm^{-2} was obtained with a MEA consisting of photo-printed Pt (0.12 mg cm^{-2}) on a Nafion membrane as the catalyst. Cyclic voltammetry measurements in solutions containing methanol or formic acid showed that a mass-specific methanol oxidation current of 197 mA mg^{-1} Pt could be achieved and that the co-deposition of Pd with Pt lowered the formic acid oxidation potential in addition to reducing the formation of the "poisonous" intermediate CO_{ads}.

Keywords: Photographic printing; Pt deposition; Nano-particle; Catalyst; Fuel cell

1. Introduction

Most current technologies for the fabrication of low temperature fuel cells, such as H_2 proton exchange membrane fuel cells (PEMFCs) and direct methanol fuel cells (DMFCs), rely on the incorporation of layers of ink-based noble metal catalysts near the polymer electrolyte membrane [1]. In order to meet the efficiency, durability and cost requirements for fuel cells, research and development have been focused on identifying less expensive new catalyst materials, minimizing precious metal loading, improving component durability and developing novel, low cost and high volume fabrication methods for the membrane electrode assembly (MEA). The demand for portable power is rising due to the increasing number of wireless electronic devices in our life. Miniaturized fuel cells have significant advantages over conventional batteries because of a longer life time, a higher power density and instantaneous recharging. In order for miniaturized fuel cells to be easily integrated into many portable electronic devices and to minimize the production costs, the future miniaturized fuel cell design needs to be compatible with the current Si-based integrated circuit processing technology [2]. Therefore, a catalyst production method that is compatible with the advanced silicon processing, such as photolithography, will be advantageous.

Pt printing is one of the oldest photographic processes, which was developed by William Willis in 1873 [3,4]. Today Pt printing is an option for printers and photographers when image quality and archival permanence are paramount considerations.

In a typical Pt printing process, the Pt salt is not light sensitive. Instead, a sensitizer, e.g. ferric oxalate $Fe_2(C_2O_4)_3$, is the light sensitive component and contains iron in the ferric state (Fe^{3+}) that easily accepts an electron to change to the ferrous state (Fe^{2+}) under UV radiation (Eq. (1)) via a radical-anion mechanism [6]. The reduced Fe^{2+} serves as the reducing agent in the development step, reaction (Eq. (2)), which is also called the Berkeley reaction [4]. The Pt ions in the precursor salt are reduced by the redox reaction (Eq. (2)) and nano-scaled Pt metal particles are deposited onto photographic paper to form black and white images. Developers, such as potassium oxalate, ammonium citrate or sodium citrate, increase the solubility of $Fe(C_2O_4)$ by complexation and permit the Pt producing redox reaction (Eq. (2)) to take place [5]. The development process

* Corresponding author. Tel.: +1 574 631 7605; fax: +1 574 631 8366.
E-mail address: jjiang@nd.edu (J. Jiang).

0378-7753/$ – see front matter © 2006 Elsevier B.V. All rights reserved.
doi:10.1016/j.jpowsour.2006.07.026

in Pt printing includes particle nucleation and growth, which is exactly the same as producing metal particles by other chemical reduction methods. Not only Pt, but other noble metals, such as Pd, Rh, Ir and Au, can be deposited based on the same principle.

The reactions taking place in the process are shown below,

$$Fe_2(C_2O_4)_3 \xrightarrow{\text{UV light}} 2Fe(C_2O_4) + 2CO_2 \quad (1)$$

$$6Fe(C_2O_4) + 3K_2PtCl_4 \xrightarrow{\text{developer}} 2Fe_2(C_2O_4)_3 + 2FeCl_3 + 6KCl + 3Pt \quad (2)$$

Potassium tetrachloroplatinate(II) was chosen as the Pt precursor salt instead of hydrogen hexachloroplatinate(IV) due to the relative faster kinetics of the Pt producing reaction, shown in Eq. (2) [5]. The residue Fe^{3+} and excess Fe^{2+} ions are washed from the paper with ethylenediaminetetraacetate (EDTA) and water.

Matsumoto [7] proposed that this Pt printing process could be an alternative way to prepare catalysts, such as Pt, on different substrates for applications such as oil refining, automotive catalytic converters and fuel cells. Even though he demonstrated the capability of deposition of 100 nm Pt on substrates, such as PEEK or Nafion, by simply repeating this well-known Pt photographic procedure, the catalytic activity of the Pt deposits was never studied. In this paper, we have investigated the catalytic activity of the photographically deposited Pt for H_2 and methanol oxidation reactions using a PEM fuel cell and an ordinary three-electorde electrochemical cell. The catalytic behavior of photographically deposited Pd/Pt alloys for the formic acid oxidation reaction was also studied. The advantages and disadvantages of this novel catalyst preparation method are discussed.

2. Materials and methods

2.1. Photographic deposition process

Unless otherwise specified, all of the chemicals were purchased from Bostick & Sullivan, Santa Fe, NM, USA. For Pt printing, a 0.48 M aqueous solution of potassium tetrachloroplatinate (K_2PtCl_4) was used as the Pt precursor salt solution. For Pd printing, a solution consisting of 0.56 M $PdCl_2$ and 1.54 M NaCl (Fisher Scientific, Pittsburg, PA, USA) was the Pd precursor salt solution. The UV sensitizer was 0.73 M ferric oxalate ($Fe_2(C_2O_4)_3$). To make the photographic emulsion, equal volumes of the above metal precursor solution (K_2PtCl_4 solution or Na_2PdCl_4 solution) and the sensitizer $Fe_2(C_2O_4)_3$ were mixed together. Depending on the catalyst surface loading desired, a measured amount of emulsion was applied to the substrate to be printed, spread by a glass rod and air-dried. The coated substrate was then exposed to a mercury lamp UV light source with an exposure intensity of 2 mW cm^{-2} and the primary exposure wavelength of 350–500 nm for 5 min. After exposure, the substrate was developed in 0.5 L of 1.1 M ammonium citrate $(NH_4)_2HC_6H_5O_7$ for 10 min. Finally, the Pt-coated substrate was washed with 500 mL of a 9 wt% EDTA aqueous solution for half an hour, slightly agitated, and followed by three cycles of wash with 500 mL Millipore water (Millipore, Bedford, MA, USA) for 30 min each time. The prepared samples were stored in Millipore water until use.

The substrates used for printing included Toray carbon paper (TGPH-060, thickness = 0.17 mm, E-TEK Inc., Somerset, NJ, USA) and Nafion 117 membrane (Nuvant System Inc., Chicago, IL, USA). Before use, the Nafion membrane was cleaned in turn in 90 °C 3% H_2O_2, 90 °C 1 M H_2SO_4 and 90 °C Millipore water for 1 h each. This cleaning cycle was repeated at least three times and the cleaned Nafion membrane was stored in Millipore water.

The mass of Pt or Pd was analyzed by inductively coupled plasma-optical emission spectroscopy (ICP-OES) (Optima 3300XL, Perkin-Elmer, Wilton, CT, USA) after dissolving the Pt or Pd from the substrates in aqua regia.

2.2. SEM and TEM analyses

Scanning electron microscope (SEM) images were taken with a Hitachi S4500 field emission SEM (Hitachi, Tokyo, Japan). Transmission electron microscope (TEM) images were taken by using a JEOL 2100 TEM (JEOL USA Inc., Peabody, MA, USA) and the cross-section sample was microtomed by a RMC MT-X Ultramicrotome (Boeckeler Instruments Inc., Tucson, AZ, USA).

2.3. Electrochemical studies of photographically deposited metals for methanol oxidation reaction and formic acid oxidation reactions

A three-electrode electrochemical cell (Voltalab® C145/170, Hach Company, Loveland, CO, USA) was used with a SCE reference electrode and a Pt disk counter electrode. For methanol oxidation measurements, cyclic voltammetry (CV) scans (from −0.25 to 1.25 V versus SCE, with a 20 mV s^{-1} scan rate at ambient temperature) in a solution of 0.5 M H_2SO_4/1 M CH_3OH were preformed on each sample. For formic acid oxidation measurements, the solution was changed to 0.1 M HCOOH/0.5 M H_2SO_4. The working electrode held a disk sample with a silicone rubber washer to define the actual exposed area. When the Pt-coated carbon paper was tested, a graphite disk was put at the back of the carbon paper to prevent the solution from permeating through the carbon paper and reaching the stainless steel current collector on the backside. For a Pt-printed Nafion membrane, a circular disk (0.5 in. diameter) was punched and hot-pressed with a piece of carbon black ink (1 mg cm^{-2} carbon loading) coated carbon paper at 120 °C, with a pressure of 1600 lb in^{-2} for 3 min, with the catalysts facing the carbon ink side. The carbon paper served as both the current collector and a porous diffuser medium through which the electrolyte could penetrate. The working electrode assembly is shown in Fig. 1.

2.4. H_2 PEMFC performance test for Pt-printed Nafion membrane

The performance of the Pt-coated Nafion membrane was evaluated with a Scribner 890C load system controlled by FuelCell

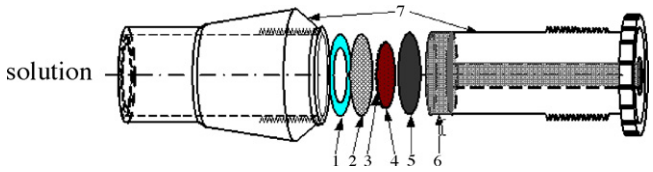

Fig. 1. Schematic view of the working electrode assembly for the three-electrode electrochemical cell. (1) Silicone rubber washer with a center circular opening of 6.35 mm diameter; (2) porous carbon paper (15 mm diameter) with carbon ink painted on the side facing the Nafion membrane; (3) Pt (or Pd) catalyst deposited photographically; (4) Nafion membrane (12.7 mm diameter); (5) graphite disk; (6) stainless steel current collector; (7) Teflon holder.

for Windows™ software (Scribner Associates Inc., Southern Pines, NC, USA). A single cell (Electrochem Inc., Wobum, MA, USA) with 5 cm^2 active area was used.

The gas diffusion layer (GDL) was carbon black ink painted Toray carbon paper (TGPH-060) with a carbon black (stock #39723, Alfa Aesar, Ward Hill, MA, USA) loading of 1.0 mg cm^{-2}. The carbon black ink was prepared by suspending 400 mg carbon black powder in 0.8 mL 5 wt% Nafion ionomer solution (Aldrich, Milwaukee, WI, USA) and 15 mL methanol. The gas diffusion electrode (GDE) was made by air-spraying Johnson–Matthey (JM) Pt catalyst (HiSPEC 1000, Alfa Aesar, Ward Hill, MA, USA) onto a GDL. The Pt ink was prepared by adding 300 mg Pt black, 1.21 mL Nafion ionomer solution into 7 mL methanol and 7 mL isopropanol. The actual loading of sprayed Pt on the GDE was 0.83 mg cm^{-2} (ICP-OES confirmed). The MEAs were hot-pressed at 120 °C under 1600 lb force for 3 min. Prior to the polarization tests, all MEAs were pre-humidified overnight in a 100% relative humidity (RH) H_2 purge on both anode and cathode sides. All cells were operated with pure H_2 and pure O_2 at flow rates of 0.2 and 0.4 L min^{-1}, respectively. The gases were fully humidified to 100% RH prior to entering the cell. Both anode and cathode were at ambient pressures.

The tested membrane electrode assemblies are shown in Fig. 2, including: (I) a non-Pt-printed Nafion 117 membrane hot-pressed between two GDEs; (II) a one-side Pt-printed Nafion 117 membrane with Pt as the anode side catalyst hot-pressed between a GDL (anode side) and a GDE (cathode side); (III) a double-side Pt-printed Nafion 117 membrane hot-pressed between two GDEs. They are denoted as type I, type II and type III MEAs in the later discussion.

During the electrochemical area (ECA) and H_2 crossover measurements, a Gamry PCI4/750 potentiostat (Gamry Instruments, Warminster, PA, USA) was used and the working electrode side was purged with N_2, and the counter electrode side was purged with H_2. The potential of the cathode was swept by means of a linear potential scan at a rate of 2 mV s^{-1} from 0.05 to 0.6 V for H_2 crossover measurements. CV measurements from 0 to 0.8 V at 40 mV s^{-1} were conducted to obtain the ECAs.

3. Results and discussion

3.1. SEM and TEM analyses of photographically printed Pt on different substrates

Fig. 3 shows the SEM images of Pt deposited on carbon paper and Nafion membrane. The Pt theoretical loading, real loading and deposition efficiency for these samples are listed in Table 1. A lower surface loading of Pt was observed when Pt was deposited on carbon paper, even though the theoretical loadings of both samples were about the same (Table 1). ICP-OES results confirmed that the deposition efficiency (real loading divided by the theoretical loading) on carbon paper was only 2% compared to 16% when deposited on Nafion membranes. Kim et al. [8] recently prepared palladinized Nafion membranes by a so called "ion exchange and chemical reduction" method. They stated that the Nafion membrane can be impregnated with metal nano-particles by ion exchanges of metal precursor ions with counter ions of the SO_3^- group, e.g. H^+. Therefore, the improved retention of Pt on Nafion membranes could be explained by this mechanism. It was also found that the Pt deposits on the Nafion membrane were of more uniform size than on carbon paper. According to the SEM images, the average size of the Pt deposits on the Nafion was 286 ± 51 nm, while on carbon paper the size deviation was larger, 245 ± 197 nm. TEM images of the cross-section of a Pt-printed Nafion membrane (Fig. 4) revealed that the Pt deposits in the membrane were actually clusters of Pt particles of less than 5 nm. Also, Pt has been deposited not only

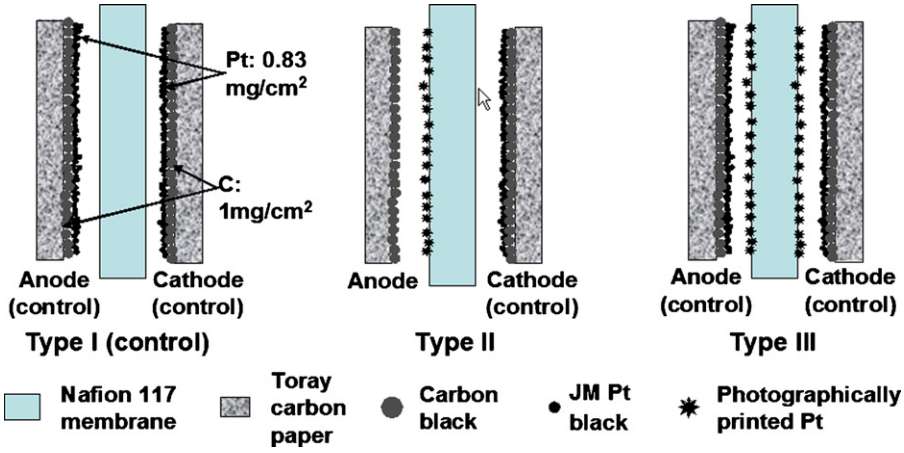

Fig. 2. MEA configurations for H_2 PEM fuel cells.

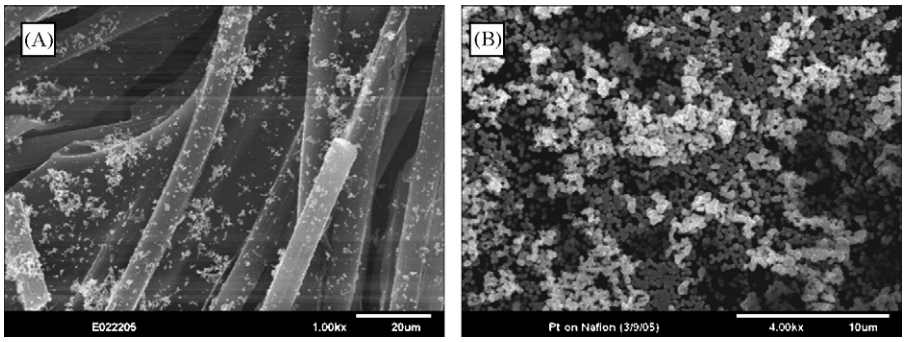

Fig. 3. SEM images of Pt photographically printed on: (A) carbon paper (1 k×) and (B) Nafion membrane (4 k×).

Table 1
Pt surface loadings and mass-specific current density of photo-printed Pt and JM Pt

Sample	Pt theoretical loading ($mg\,cm^{-2}$)	Pt real loading measured by ICP ($mg\,cm^{-2}$)	Deposition efficiency (%)	Peak methanol oxidation current density ($mA\,cm^{-2}$)	Mass-specific current density ($mA\,mg^{-1}$)
Pt-Nafion	1.25	0.2	16	11	55
Pt-carbon paper	1.5	0.03	2	5.9	197
JM Pt black	0.98	0.69	70	31.6	45.8

on the surface but inside the membrane as well. The deposition of metal catalysts inside the membrane has been seen by other researchers when they deposited metals by impregnation and chemical reduction methods [8–10]. However, in this process metal particles were formed at more than 100 μm into the membrane within half an hour coating using microliters of metal ion precursor emulsion as opposed to the 12 h soaking in the metal precursor used by Fujiwara et al. [9].

3.2. Cyclic voltammetry study of catalytic activity for methanol oxidation reaction

CV curves of typical Pt catalysts photo-printed on a Nafion membrane and carbon paper (CP) in 1 M methanol/0.5 M H_2SO_4 are shown in Fig. 5. The Pt theoretical loading, the ICP-OES measured Pt real loading, the methanol oxidation peak current densities and the mass-specific current densities of these two samples are listed in Table 1. The mass-specific current density is calculated by dividing the current density by the ICP Pt loading. When Nafion was used as a substrate, a higher methanol oxidation current density was obtained compared to the sample with carbon paper as the substrate due to the higher real loading of Pt. Owing to the exceptionally low loading of photo-printed Pt on carbon paper, a mass-specific current density of 197 $mA\,mg^{-1}$ Pt was obtained as compared to 55 $mA\,mg^{-1}$ Pt on the Nafion membrane and 45.8 $mA\,mg^{-1}$ Pt of the JM commercial Pt catalyst (Table 1). The strong adhesion of Pt particles to the Nafion membrane resulted in a stable methanol oxidation current even after the sample was stored in Millipore water for 4 weeks (Fig. 5).

3.3. Cyclic voltammetry study of catalytic activity of Pt/Pd mixtures for formic acid oxidation reaction

It has been reported that Pt-Pd alloy catalysts can enhance the rate of formic acid electrooxidation via a direct reaction mechanism and inhibit the formation of CO_{ads} [11,12]. Compared to DMFC, a direct formic acid—oxygen fuel cell has a higher

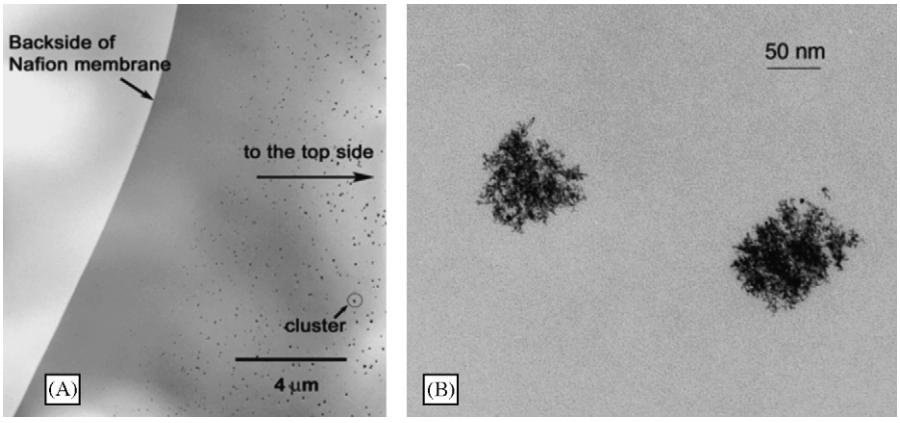

Fig. 4. TEM images of Pt aggregates inside the Nafion membrane at low (A) and high (B) magnifications.

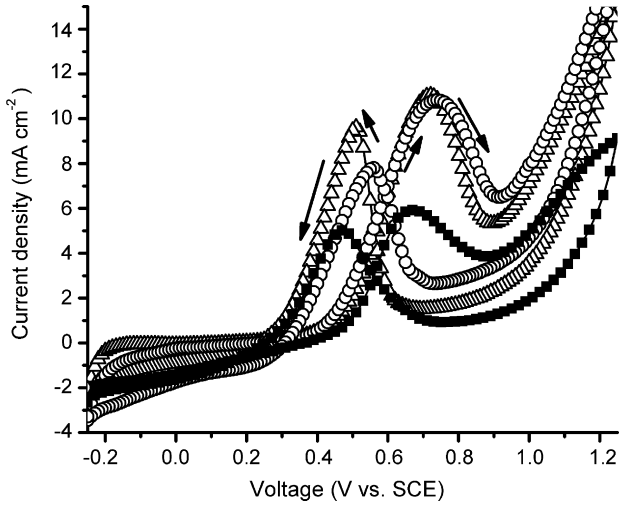

Fig. 5. CV curves (the 20th cycle) of Pt-printed carbon paper (■) and Pt-printed Nafion membranes: as produced (△) and after storing in Millipore water for 4 weeks (◯). The testing solution was 0.5 M H_2SO_4/1 M CH_3OH and the scan rate was 20 mV s^{-1}.

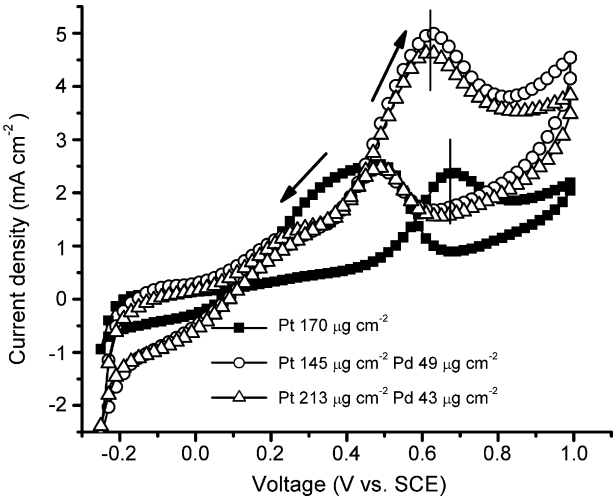

Fig. 6. CV curves (the 20th cycles) of Pt (■) and Pt/Pd mixtures (◯, △) printed on Nafion membranes in a test solution of 0.1 M HCOOH/0.5 M H_2SO_4 at a scan rate of 20 mV s^{-1}. The legend lists the real loadings of Pt and Pd for each sample.

theoretical open circuit potential (1.45 V versus 1.23 V at room temperature), reduced fuel crossover and faster room temperature kinetics [12,13]. In this study, Pd was deposited with Pt on Nafion membranes by photographic printing from a mixed Pd-Pt emulsion. The deposition efficiency was analyzed by ICP and the results are listed in Table 2. A higher surface retention was obtained for Pd than for Pt when they were co-deposited.

Fig. 6 shows that the formic acid oxidation peak (the forward peak) for pure Pt occurred at a higher potential than those of the samples with Pd, which indicates that the addition of Pd facilitates the reaction and lowers the activation energy of the reaction. Also the CO oxidation stripping peaks (the reverse peak) of samples with Pd are much smaller than that of pure Pt, indicating the inhibition of the formation of the "poisonous" CO_{ads} on the catalyst because of the presence of Pd. The formic acid oxidation current was also increased by the addition of Pd.

3.4. Performance evaluation using a single H_2 fuel cell

3.4.1. H_2 crossover

To experimentally determine the H_2 crossover, linear sweep voltammetry (LSV) was performed while the cathode side of the fuel cell was purged with N_2 and the anode side was purged with H_2. The output limiting current was used to derive the H_2 crossover flux from Faraday's law. Typical results of such experiments are shown in Fig. 7. Two type II MEAs are compared with one type I MEA, which was used as a control in the studies. Based on the calculations, the rate of H_2 crossover for the type I MEA through a non-Pt-printed Nafion 117 membrane was 2.3×10^{-9} mol s^{-1} cm^{-2}. While the H_2 crossover rates for type II MEAs were 1.63×10^{-9} and 1.32×10^{-9} mol s^{-1} cm^{-2} when the printed Pt loadings were 0.08 and 0.16 mg cm^{-2}, respectively. After Pt was printed on the Nafion membrane, the H_2 crossover was slightly decreased. In a real fuel cell operation conditions, Watanabe et al. have already found [14–16] that by incorporating nano-sized, dispersed Pt particles inside the Nafion membrane, H_2 crossover was reduced due to the catalytic oxidation of crossover hydrogen with oxygen on Pt particles within the membrane. In the meantime, Watanabe et

Table 2
ICP analyses of the actual loadings of photo-printed Pt and Pt/Pd mixtures

Sample ID	Theoretical loading (mg cm^{-2})	Real loading (mg cm^{-2})	Deposition efficiency (%)
1	Pt: 1	Pt: 0.17	17
2	Pt: 0.9 Pd: 0.1	Pt: 0.213 Pd: 0.043	Pt: 24 Pd: 43
3	Pt: 0.8 Pd: 0.2	Pt: 0.145 Pd: 0.049	Pt: 18 Pd: 25

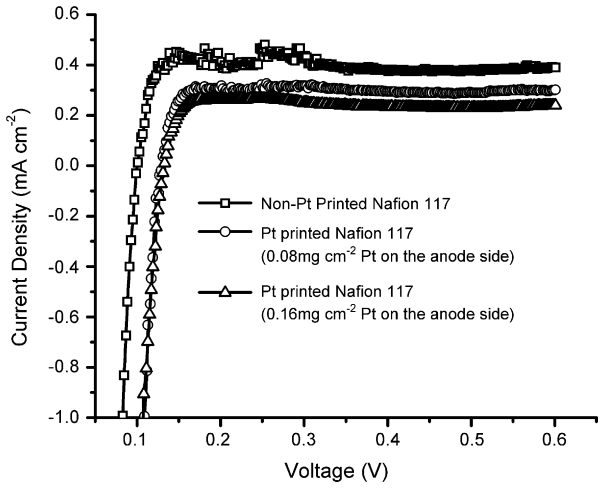

Fig. 7. Linear sweep voltammograms for the type I MEA containing non-Pt-printed Nafion 117 membrane (□) and two type II MEAs containing Pt-printed Nafion 117 membrane with 0.08 mg cm^{-2} Pt (◯) and Pt-printed Nafion 117 membrane with 0.16 mg cm^{-2} Pt (△), respectively. The temperatures of the anode humidifier/cell/cathode humidifier were 40/40/40 °C, respectively. The flow rates of H_2/N_2 were 0.2/0.2 L min^{-1}.

al. [14–16] also pointed out that the reaction-generated water self-humidified the membrane and allowed the fuel cell to work without any humidification. Our photographic printing process also deposited some Pt particles inside the membrane as shown previously in the TEM images. Even though this portion of the Pt particles may not be able to serve as the catalysts for the electrode reactions, they could still perform as proposed by Watanabe by suppressing H_2 crossover and thereby humidifying the membrane.

3.4.2. Electrochemical area

The ECA of the Pt catalyst can be calculated from the charge for proton reduction based on the well-established quantity for the charge needed to reduce a monolayer of protons on Pt ($210\,\mu C\,cm^{-2}$ Pt) [17]. If the Pt loading of the electrode is known, the mass-specific electrochemical area can be obtained from cyclic voltammetry data. During measurements, the working electrode side was purged with humidified N_2 and the other side was purged with humidified H_2. Integration of the proton reduction peak as shown in Fig. 8A, yielded the reduction charge of 86.27 and 0.27 mC for the loading of $0.83\,mg\,cm^{-2}$ Johnson–Matthey Pt black and $0.16\,mg\,cm^{-2}$ photographically printed Pt, respectively. Therefore, the ECA for the above catalysts are 10.3 and $0.16\,m^2\,g^{-1}$ Pt. The lower ECA of the printed Pt is probably due to the deposition of Pt inside the membrane and the aggregation of Pt particles as shown in the TEM images.

3.4.3. Ionic resistance

The ionic resistance of the membrane was measured by a current interrupt method provided by the Scribner load system and FuelCell^{TM} software. The calculation was based on the assumption that the electronic ohmic resistances associated with the cell electrodes, gas diffusion layers, current collectors, leads as well as contact resistances between these components, are much smaller than the ohmic resistance due to the ion transport through the polymer membrane electrolyte. Fig. 9 shows the temperature dependence of membrane conductivities for a type I MEA and a type III MEA at 100% RH. The type I MEA had a non-Pt-printed Nafion 117 membrane hot-pressed with two GDEs; while the type III MEA had a double-side Pt-printed Nafion membrane hot-pressed to two identical GDEs as in type I MEA. The total ICP loading of photographically printed Pt in the type III MEA was $0.24\,mg\,cm^{-2}$. It is clearly shown that the proton conductivity of the Pt-printed membrane is actually slightly higher than that of the non-Pt-printed membrane. Therefore, the deposition of Pt onto the Nafion membrane did not impact the proton conductivity, even though some of the Pt was deposited inside of the membrane. Similar results were also observed by Watanabe et al. [14,16]. The reason that causes this is still not clear. However, it could be due to the higher water uptake observed for the Pt-impregnated Nafion membrane over the normal Nafion membrane at the same humidification condition [16]. The "self-humidified" effect during the operation of the fuel cell as reported in Watanabe et al.'s work [14], has not been tested yet in this work. For both MEAs, the proton conductivities increase with temperature because high temperature enhances the ion transport in the membrane. Activation energies

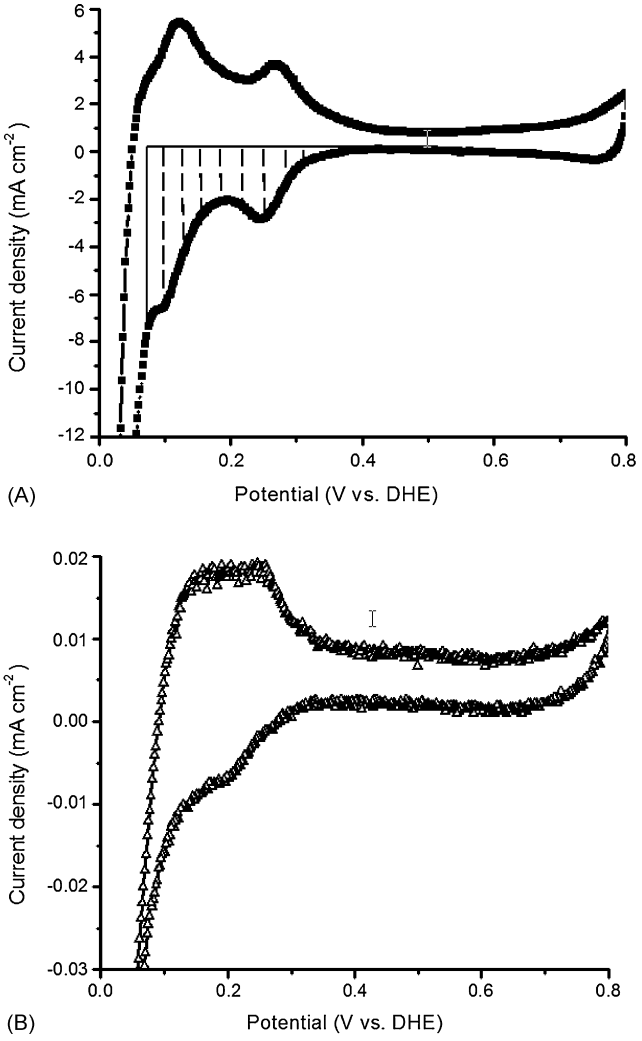

Fig. 8. CV curves of proton oxidation and reduction on: (A) Johnson–Matthey Pt black ($0.83\,mg\,cm^{-2}$) and (B) photographically printed Pt ($0.16\,mg\,cm^{-2}$). The area of the single cell: $5\,cm^2$. The temperatures of the anode humidifier/cell/cathode humidifier were 25/25/25 °C, respectively. H_2/N_2 flow rate: $0.2/0.2\,L\,min^{-1}$.

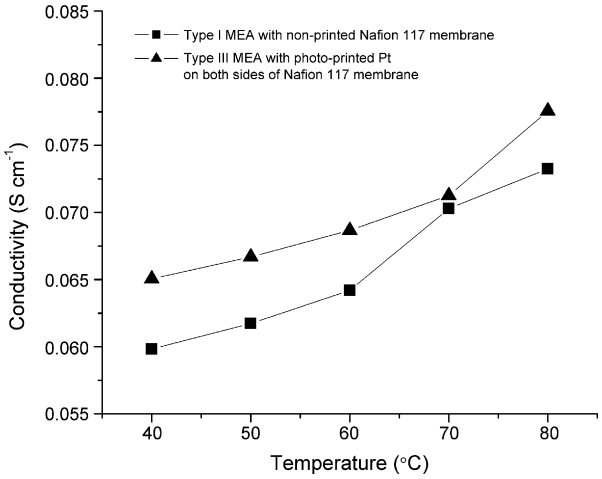

Fig. 9. Temperature dependence of membrane conductivities for the type I MEA (■) and the type III MEA (▲) measured by the current interrupt method. The loading of photographically printed Pt on both sides of the type III MEA was $0.24\,mg\,cm^{-2}$ totally. All data were collected under 100% RH.

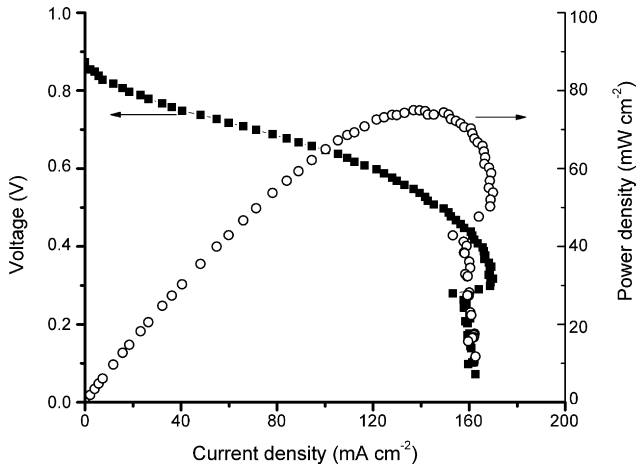

Fig. 10. Typical H_2 PEMFC performance data at 60 °C for the type II MEA. The total loading of the photographically deposited Pt on the anode side was 0.12 mg cm^{-2}. The flow rates of humidified H_2 and O_2 were 0.2 and 0.4 L min^{-1}, respectively. No backpressure was applied.

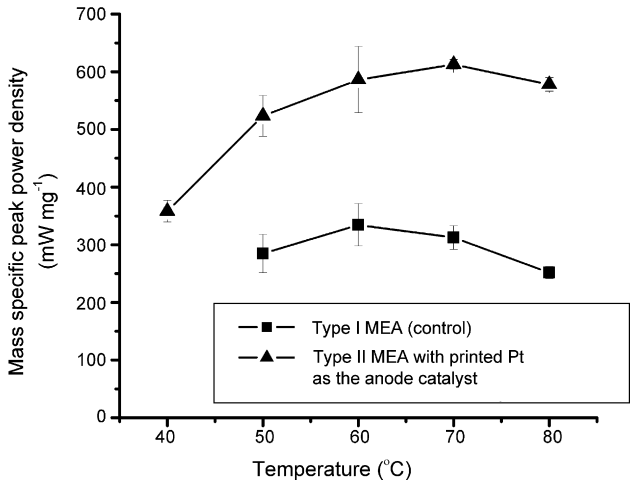

Fig. 11. The dependence of mass-specific peak power density on cell temperature for type I MEA with JM Pt as the anode catalyst (■) and type II MEA with photo-printed Pt as the anode catalyst (▲). The flow rates of humidified H_2 and O_2 were 0.2 and 0.4 L min^{-1}, respectively. No backpressure was applied.

ranging from 1 to 20 kJ mol^{-1} have been reported for Nafion 117 membranes in our working temperature range [18]. Using the Arrhenius equation, the activation energies for type I and type III MEAs have been calculated to be 3.8 and 4.9 kJ mol^{-1}, respectively.

3.4.4. H_2 fuel cell performance based on the Pt-printed Nafion membrane

The performance data of a typical type II MEA containing photographically deposited Pt of 0.12 mg cm^{-2} as the anode side catalyst is shown in Fig. 10. The data were collected at 60 °C, 100% relative humidity and using pure H_2 and O_2. A maximum power density of 75 mW cm^{-2} was achieved with this type of MEA. When compared to the control MEA with commercial JM Pt anode catalyst, the mass-specific peak power density (normalized by the anode Pt loading) was almost doubled (Fig. 11). However, for type II MEA with photo-printed Pt catalyst, the polarization curve in Fig. 10 shows a clear mass transport limited region with a mass transport limiting current of 163 mA cm^{-2}. The reason for this mass limiting region at higher currents, is considered to be the limited catalyst ECA resulting from the aggregation of the Pt particles and partial deposition of the catalyst inside of the membrane. Therefore, the accessible catalytic surface area for the fuel is low. This inefficient catalyst utilization has also been reported for production of Pt onto Nafion membranes by the "impregnation–chemical reduction" method due to Pt being deposited in the membrane, which results in insufficient accessibility of the reactants and electronic contact [9,10].

3.5. Patterning of Pt catalyst layer by photographic printing

To demonstrate the potential application of this catalyst deposition method in micro-fuel cells, some micron size patterns have been generated using this process. Fig. 12 displays two platinized flow fields and one pair of platinized interdigitated electrodes photographically deposited on a Nafion membrane. The flow fields have dimensions of 1 cm × 1 cm, and the overall size of the pair of interdigitated electrodes is 0.68 cm × 0.63 cm. The

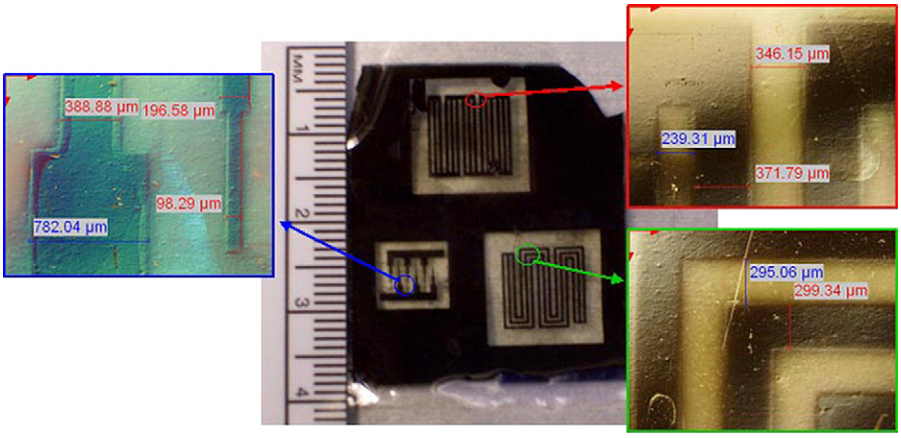

Fig. 12. Optical pictures of two triple-serpentine flow fields and a pair of interdigitated electrodes prepared by photographic printing of Pt onto the Nafion 117 membrane.

smallest feature size is 100 μm. Due to the shrinkage of the membrane after drying, the measured dry feature sizes are all smaller than the designed feature sizes. This volume change of Nafion due to the change in hydration level is one of the major problems in micro-fuel cell development. To overcome this problem, much effort has been expended to develop solid-state protonic conductors, such as acid loaded porous silicon [19]. Since this photo-printing method is not substrate selective, it is possible that it can be easily applied to the new generation of protonic conducting membranes, including polymers, inorganic–organic hybrid materials and ceramics.

4. Conclusions

A photographic printing process has been used as a catalyst preparation method for fuel cell applications, and the catalytic activities for methanol oxidation, formic acid oxidation and H_2 oxidation reactions have been evaluated by the electrochemical cyclic voltammetry method and a single H_2 fuel cell testing system.

With the current preparation conditions, Pt particles of less than 5 nm can be formed. However, they tend to form clusters up to 300 nm in size. A mass-specific methanol oxidation current density of up to 197 mA mg^{-1} Pt was achieved with the photographic deposited Pt onto carbon paper. A much higher deposition efficiency was found when Pt was deposited directly onto Nafion membranes. The catalyst deposits on Nafion membranes exhibited excellent adhesion and the mass-specific methanol oxidation current was comparable to the commercial JM Pt. A PEMFC test of the MEA containing 0.12 mg cm^{-2} photographically deposited Pt on the Nafion membrane provided a peak power density of 75 mW cm^{-2}. This photographic method can also be used to prepare other noble metal catalysts such as Pd and its alloys. Experimental results showed that the co-deposition of Pd with Pt resulted in a lower formic acid oxidation potential and a reduced formation of CO_{ads}.

The photographic printing method was shown to be compatible with photolithographic processes used in integrated circuit fabrication and thus could be a promising candidate process for catalyst formation in the manufacturing of miniaturized fuel cells. In addition, the process itself does not have any substrate type limitation.

Currently the major problems with this method are its low deposition efficiency and particle aggregation. These issues will be addressed through adjustments of emulsion chemistry and process conditions.

Acknowledgements

The research described herein was supported by the Indiana 21st Century Research and Technology Fund (contract number 910,010,465) and the U.S. Army CECOM RDEC through Agreement DAAB07-03-3-K414. Such support does not constitute endorsement by the U.S. Army of the views expressed in this publication. The authors want to thank the Center for Environmental Science and Technology for the use of ICP-OES, Dr. William Archer for the help in TEM sample preparation and Prof. Thomas Kosel for the use of the TEM.

References

[1] S.S. Kocha, in: W. Vielstich, H.A. Gasteiger, A. Lamm (Eds.), Handbook of Fuel Cells: Fundamentals, Technology, and Applications, vol. 3, John Wiley & Sons Ltd., Chichester, England, 2003, pp. 538–565.
[2] J.P. Meyers, H.L. Maynard, J. Power Sources 109 (2002) 76–88.
[3] W.D.W. Abney, L. Clark, Platinotype, Scovill and Adams, New York, 1898, p. 7.
[4] D. Arentz, Platinum and Palladium Printing, Focal Press, Boston, 2000, p. 4.
[5] M.J. Ware, J. Photogr. Sci. 34 (1986) 13–25.
[6] G.D. Cooper, B.A. DeGraff, J. Phys. Chem. 75 (1971) 2879–2902.
[7] R. Matsumoto, US Patent 5,686,150 (1997).
[8] Y.J. Kim, W.C. Choi, S.I. Woo, W.H. Hong, Electrochim. Acta 49 (2004) 3227–3234.
[9] N. Fujiwara, K. Yasuda, T. Ioroi, Z. Siroma, Y. Miyazaki, Electrochim. Acta 47 (2002) 4079–4084.
[10] S.-A. Sheppard, S.A. Campbell, J.R. Smith, G.W. Lloyd, T.R. Ralph, F.C. Walsh, Analyst 123 (1998) 1923–1929.
[11] M. Arenz, V. Stamenkovic, T.J. Schmidt, K. Wandelt, P.N. Ross, N.M. Markovic, Phys. Chem. Chem. Phys. 5 (2003) 4242–4251.
[12] C. Rice, S. Ha, R.I. Masel, A. Wieckowski, J. Power Sources 115 (2003) 229–235.
[13] R.S. Jayashree, J.S. Spendelow, J. Yeom, C. Rastogi, M.A.K. Shannon, P.J.A. Kenis, Electrochim. Acta 50 (2005) 4674–4682.
[14] M. Watanabe, H. Uchida, M. Emori, J. Electrochem. Soc. 145 (1998) 1137–1141.
[15] M. Watanabe, H. Uchida, H. Igarashi, Macromol. Symp. 156 (2000) 223–230.
[16] M. Watanabe, H. Uchida, Y. Seki, M. Emori, J. Electrochem. Soc. 143 (1996) 3847–3852.
[17] K. Kinoshita, P. Stonehart, in: J.O.M. Bockris, B.E. Conway (Eds.), Modern Aspects of Electrochemistry, vol. 12, Plenum Press, New York, 1977, pp. 183–266.
[18] M. Doyle, G. Rajendran, in: W. Vielstich, H.A. Gasteiger, A. Lamm (Eds.), Handbook of Fuel Cells: Fundamentals, Technology and Applications, vol. 3, John Wiley & Sons Ltd., Chichester, England, 2003, pp. 351–395.
[19] S. Gold, K.L. Chu, C. Lu, M.A. Shannon, R.I. Masel, J. Power Sources 135 (2004) 198–203.